# Improvement of Critical Temperature of Superconducting NbTiN and NbN Thin Films Using the AlN Buffer Layer

**Tatsuya Shiino, Shoichi Shiba, and Nami Sakai**

Department of Physics, The University of Tokyo, Hongo, Bunkyo-ku, Tokyo 113-0033, Japan

E-mail: `shiino@taurus.phys.s.u-tokyo.ac.jp`

**Tetsuya Yamakura**

Institute of Physics, Graduate School of Pure and Applied Sciences, University of Tsukuba, Ten-nodai, Tsukuba, Ibaraki 305-8577, Japan

**Ling Jiang**

College of Information Science and Technology, Nanjing Forestry University, Nanjing 210037, Jiangsu, China

**Yoshinori Uzawa**

National Astronomical Observatory of Japan, Osawa, Mitaka, Tokyo 181-8588, Japan

**Hiroyuki Maezawa**

Solar-Terrestrial Environment Laboratory, Nagoya University, Furo-cho, Chigusa-ku, Nagoya 464-8602, Japan

**Satoshi Yamamoto**

Department of Physics, The University of Tokyo, Hongo, Bunkyo-ku, Tokyo 113-0033, Japan

**Abstract.** Thin superconducting NbTiN and NbN films with a few nm thickness are used for various device applications including hot electron bolometer mixers. Such thin films have lower critical temperature ($T_c$) and higher resistivity than corresponding bulk materials. To improve them, we have investigated an effect of the AlN buffer layer between the film and the substrate (quartz or soda lime glass). The AlN film is deposited by DC magnetron sputtering, and the process condition is optimized so as that the X-ray diffraction intensity from the 002 surface of Wurtzite AlN becomes highest. By use of this well-characterized buffer layer, $T_c$ and resistivity of the NbTiN film with a few nm thickness are remarkably increased and decreased, respectively, in comparison with those without the buffer layer. More importantly, the AlN buffer layer is found to be effective for NbN. With the AlN buffer layer, $T_c$ is increased from 7.3 K to 10.5 K for the 8 nm NbN film. The improvement of $T_c$ and resistivity originates from the good lattice matching between the 002 surface of AlN and the 111 surface of NbTiN or NbN, which makes better crystallization of the NbTiN or NbN film. This is further confirmed by the X-ray diffraction measurement.

PACS numbers: 74.78.-w

Submitted to: *Supercond. Sci. Technol.*

## 1. Introduction

Superconducting hot electron bolometer (HEB) mixers are now used as the most sensitive heterodyne detectors to observe faint THz signals particularly for astronomical and atmospherical studies.[1, 2] In the case of the phonon-cooled HEB mixers,[3] a superconducting film should be as thin as a few nm for rapid and efficient cooling of hot electrons caused in the mixing process. As superconducting materials, NbN or NbTiN is usually used. Although these materials have high critical temperature ($T_c$) of about 16-18 K for the bulk case,[4, 5] $T_c$ of a thin film tends to be much lower than that.[6] In addition, the resistivity of these materials becomes higher for a thinner film. Since high $T_c$ is preferable for good performance of the HEB mixers, it is important to realize a thin superconducting film with high $T_c$. Furthermore, low resistivity is required in order to maximize an effect of the diffusion-cooling used supplementarily in addition to the phonon-cooling, because such a 'combination' cooling would be a potential direction for further improvements of the HEB mixer performance.[7, 8]

The most fundamental way to obtain high quality superconducting films is the epitaxial growth on substrates. In this case, the lattice structure of the film material should well match with that of the substrate, as in the case of NbN on the MgO substrate.[9] Because of this reason, the substrate choice is strongly limited, which sometimes restricts a range of applications. It is therefore important to develop a practical way to improve the film quality regardless of substrates. One is to heat the substrate up to a few hundred degree centigrade during the sputtering process, because the higher temperature deposition promotes better crystallization of the film. This is successfully applied to the NbTiN and NbN films.[10, 11] Although this technique is very effective, it would sometimes restrict the HEB device fabrication process. For instance, the lift-off process is difficult to be applied, because the resist cannot survive in good conditions at very high temperature. Another way is to introduce a buffer layer between a superconducting film and a substrate, which improves their lattice matching. For instance, the AlN buffer layer is reported to be effective for the NbTiN film.[12, 13] However, the effect of the buffer layer has not been discussed on the basis of its characterization. In the present study, we have focused on this technique, and have carefully examined the role of the AlN buffer layer not only for NbTiN but also for NbN. In all the experiments described below, quartz ($SiO_2$ z-cut) substrates or simple soda lime glass substrates are employed, although the quartz substrates are used for the HEB mixer fabrication.

## 2. Preparation of AlN Film

The AlN film was fabricated on a quartz wafer or a glass wafer by the reactive DC magnetron sputtering of the Al target under atmosphere of the gaseous mixture of Ar and $N_2$ at the room temperature. The distance from the target to the substrate is 70 mm, and the Al target size is 50 mm in diameter. Typical background pressure was $3\times10^{-6}$ Pa. When we increased the nitrogen content from zero, the deposited film gradually became transparent, and the electric conductivity of the film was rapidly lost. At the $N_2$/Ar flow ratio of 0.20, the deposited film is completely transparent and the electric conductivity is almost zero. The film shows compressive stress, according to the measurement by a surface profiler.

We employed an X-ray diffraction (XRD) method in order to characterize the crystallinity of the AlN film fabricated above. As shown in Figure 1, the XRD pattern is dominated by the 002 surface of Wurtzite-type AlN. Although AlN has two types of crystal structure, Wurtzite and Sphalerite, the diffraction due to the Sphalerite structure was not detected at all in the present study. This is probably because Wurtzite AlN is slightly more stable than Sphalerite AlN. Then we optimized the process conditions so as that the XRD intensity from the 002 surface becomes highest. When the $N_2$/Ar ratio is in the range from 0.30 to 0.35, the peak intensity from the 002 surface does not change significantly. Hence, we employed the following conditions for the AlN film fabrication; the $N_2$/Ar ratio of 0.33, the total pressure of 0.084 Pa, and the sputtering power of 100 W. Under these conditions, the deposition rate was 16.3 nm min$^{-1}$.

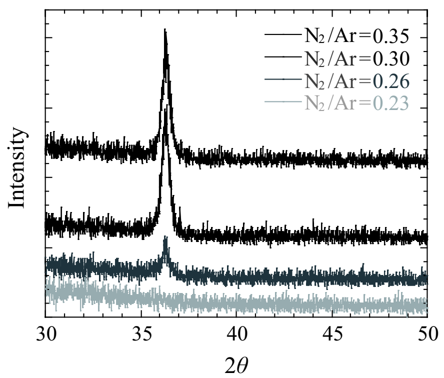


**Figure 1.** X-ray diffraction patterns of the AlN films fabricated with different $N_2$/Ar flow ratios. The thickness of the films is 90 nm.

## 3. Results for NbTiN

First, we examined the effect of the AlN buffer layer for the NbTiN film. The NbTiN film was deposited by the RF assisted DC magnetron (helicon) sputtering of the NbTi (weight ratio of Nb : Ti = 4 : 1) target under atmosphere of the gaseous mixture of Ar and $N_2$ at the room temperature.[8] The distance from the target to the substrate is 150 mm, and the size of the NbTi target is 50 mm in diameter. Typical background pressure was $3\times10^{-6}$ Pa as in the case of AlN. The sputtering conditions were the $N_2$/Ar flow ratio of 0.10, the total pressure of 0.420 Pa, and the sputtering power of 220 W. The deposition rate was 9.8 nm min$^{-1}$.

In our device fabrication system, the AlN and NbTiN films can be formed in the same sputter chamber without breaking vacuum. Therefore, we first deposited the AlN buffer layer of 20 nm on a wafer, and successively deposited the NbTiN film. In order to examine effects of the AlN buffer layer, we also deposited the NbTiN film directly on another wafer. In these deposition processes, a pattern for the 4-terminal measurement was formed by using a photo-resist mask.

The fabricated film was cooled by the 4 K GM refrigerator for the $T_c$ measurement. The wafer was mounted on a copper adaptor on the cold head of the refrigerator, and the temperature was measured by the semiconductor sensor attached to the adaptor. The resistance of the film was measured by a conventional 4-terminal method.

Figure 2 shows the R-T curve of the 8 nm thickness NbTiN film with and without the AlN buffer layer deposited on quartz wafers. Apparently, $T_c$ is higher by 2.7 K for the film with the buffer layer. In addition, the room-temperature resistivity of the film is also decreased by 20 %. Note that similar results were obtained for the AlN buffer layer with the thickness of 10 nm; the difference in $T_c$ is only within 0.3 K between the 10 nm buffer layer and the 20 nm one.

We also measured $T_c$ for the NbTiN film with various thickness. For this experiment, simple glass wafers were used as substrates. As shown in Figure 3, the increase of $T_c$ tends to be larger for the thinner film. We confirm that the increase of $T_c$ for the 8 nm film on the glass wafer is almost comparable to that for the quartz wafer shown in Figure 2. This means that the AlN buffer layer is effective regardless of the substrate.

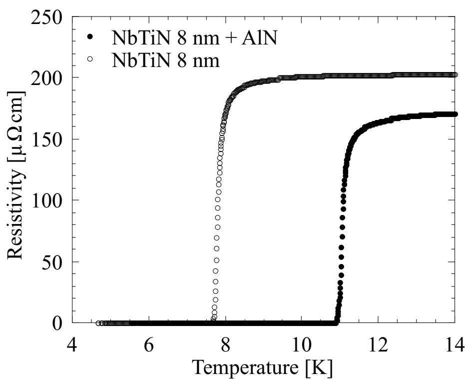


**Figure 2.** R-T curves of the NbTiN films on the quartz wafer with and without the AlN buffer layer.

## 4. Results for NbN

Since we found a significant effect of the AlN buffer layer for the NbTiN film, we also examined it for the NbN film. It is known that the NbN thin film shows a good superconductivity only when it is epitaxially formed on the MgO substrate.[9, 14] When the quartz or Si substrate is used, MgO or SiC is often employed as a buffer layer in

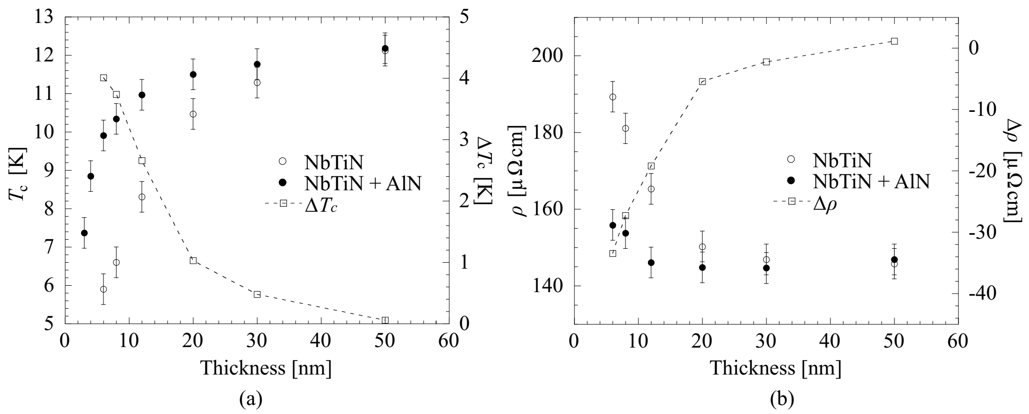


**Figure 3.** Thickness dependence of $T_c$ (a) and resistivity (b) for the NbTiN film on the glass wafer with and without the AlN buffer layer. Dashed lines represent the difference.

order to increase $T_c$.[15, 16, 11] Meledin et al. demonstrated the HEB mixer fabrication using the NbN film on the quartz substrate with the MgO buffer layer. On the other hand, the AlN buffer layer for the NbN film has not been reported, as far as we know. Since NbN has almost the same lattice constant as NbTiN, the increase and decrease of $T_c$ and resistivity, respectively, would be expected by using the AlN buffer layer.

The NbN film was deposited by the RF assisted DC magnetron sputtering of the Nb target under atmosphere of the gaseous mixture of Ar and $N_2$. The target size, the distance from target to substrate, and typical background pressure are the same as in the case of NbTiN. It is reported that $T_c$ of the NbN film is very sensitive to the $N_2$ partial pressure [9], and hence, it was optimized by measuring $T_c$ of the deposited films. The sputtering conditions of NbN were the $N_2$/Ar ratio of 0.115, the total pressure of 0.250 Pa, and the sputtering power of 250 W. The deposition rate was 11.5 nm min$^{-1}$.

As in the case of the NbTiN film, we found remarkable increase of $T_c$ by introduction of the AlN buffer layer. For the 8 nm thick NbN film on a quartz substrate, $T_c$ was increased from 7.3 K to 10.5 K (Figure 4), and the room-temperature resistivity was decreased by 20 %. Again more improvement was seen for a thinner film, as shown in Figure 5, where glass wafers were used as substrates. Our NbN film with 6 nm thickness did not show the superconducting transition even at 4 K without the buffer layer , whereas $T_c$ became as high as 10.5 K by use of the AlN buffer layer. This means that $T_c$ is increased by more than 6 K. Even for the film with 3 nm thickness, $T_c$ is about 8 K. This is comparable to the case of the MgO buffer layer ($T_c$=8.4 K for the 3-4 nm film) on the quartz substrate.[16] Note that improvements seem to be larger for the films on glass substrates than those on quartz in the case of NbN.

## 5. Discussion

In the present study, we have confirmed that the AlN buffer layer is effective for the NbTiN film, as reported previously.[12, 13] In addition, we have found, for the first

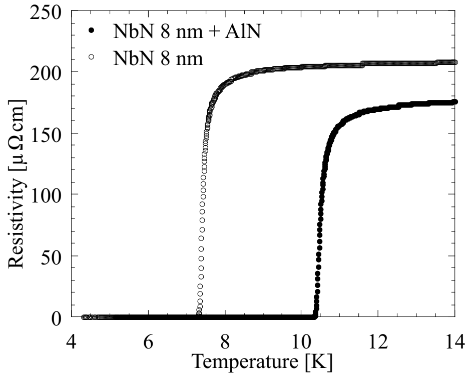


**Figure 4.** R-T curves of the NbN films on the quartz wafer with and without the AlN buffer layer.

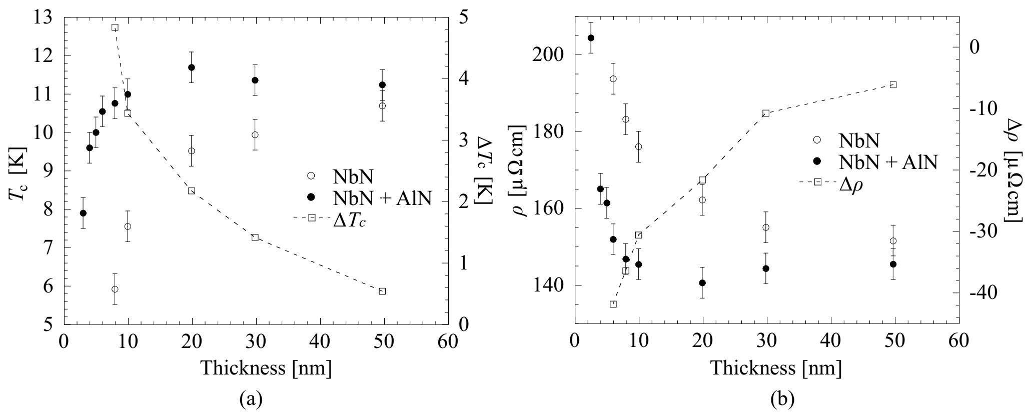


**Figure 5.** Thickness dependence of $T_c$ (a) and resistivity (b) for the NbN film on the glass wafer with and without the AlN buffer layer. Dashed lines represent the difference.

time, that it is also effective for the NbN film. This finding will increase possible choices for fabrication processes of the NbN HEB mixer. The improvement of $T_c$ and resistivity seems to originate from better crystallization of these superconducting films on the AlN buffer layer than on the bare substrate, as described below.

The buffer layer is generally used to improve the lattice matching for a superconducting material, and hence, a buffer layer should have the same lattice type and a similar lattice constant to the material in purpose. For instance, MgO is an good buffer layer for NbN and NbTiN. MgO has the NaCl type lattice whose lattice constant only differs from that of NbN by 4 %. In contrast to MgO, AlN has a completely different lattice type (Wurtzite) from NbN/NbTiN. Nevertheless, it is very effective as a buffer layer. A key to the solution is the 111 surface of NbN/NbTiN. The 111 surface of the NaCl type lattice has a hexagonal pattern, which is the same as that of the 001 surface of the hexagonal lattice including Wurtzite (Figure 6). The "lattice constant" of the 111 surface of NbN/NbTiN, which is given as $\sqrt{2}a/2$, fits to that of Wurtzite AlN almost perfectly (Table 1). The mismatch is only less than 0.2 % both for NbN and

NbTiN. Because of this fortuitous coincidence, AlN can be used as a good buffer layer for the NbN/NbTiN films.

This prediction was confirmed by two experiments. First, we measured the effects of the AlN buffer layer by changing the crystalline quality of the AlN buffer layer. As mentioned above, we can control the diffraction intensity from the 002 surface of AlN by changing the $N_2$/Ar ratio. We examined $T_c$ and resistivity of the NbN films (8 nm) for various $N_2$/Ar ratios. The results are shown in Figure 7. Judging from the XRD pattern of Figure 1, the crystallization of the AlN film appears at the $N_2$/Ar ratio of 0.26. At this point, $T_c$ and resistivity of the NbN film show drastic changes, just like a phase transition. This means that a small portion of crystallization of AlN greatly helps the epitaxial growth of the NbN film.

This is further confirmed by the XRD patterns of NbN (10 nm), AlN (20 nm), and AlN (20 nm) + NbN (10 nm), as shown in Figure 8. Both the 111 peak of NbN and the 002 peak of AlN appear around $2\theta = 36°$, because the distance between the 111 layers of NbN (0.253 nm) is almost the same as that between the 002 layers of AlN (0.249 nm). The diffraction from the 111 surface of NbN is certainly enhanced, when the AlN buffer layer is introduced.

For the HEB device application, the influence of the AlN buffer layer on the intermediate frequency bandwidth is very important, because the buffer layer may affect the escaping time of phonons from the NbN/NbTiN film to the substrate. Fabrication and evaluation of the HEB mixers using the NbTiN/AlN or NbN/AlN film are now in progress, and the influence will be studied in the near future.

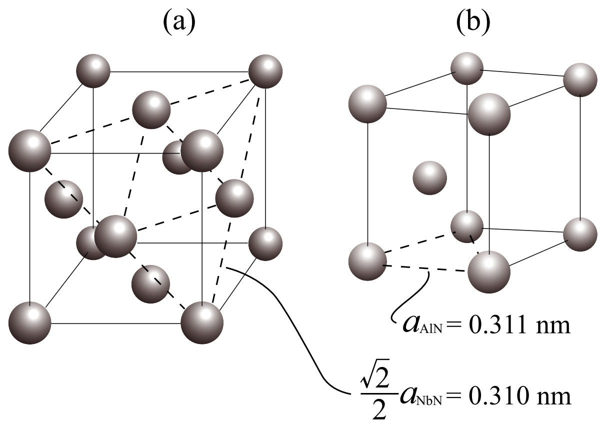


**Figure 6.** (a) The 111 surface of NbN/NbTiN. N atoms and Ti atoms are omitted. (b) The 001 surface of AlN. N atoms are omitted.

## 6. Acknowledgement

We are grateful to Dr. Shinichi Uchida and Dr. Kenji Kojima of The University of Tokyo for allowing us to use their X-ray diffractometer. We thank to Ryuta Furuya and

**Table 1.** Lattice type of NbN, NbTiN, MgO and AlN.

| | Lattice Type | Lattice Constants [nm] |
|---|---|---|
| NbN | NaCl -cubic | 0.439 |
| NbTiN | NaCl -cubic | 0.440 |
| MgO | NaCl -cubic | 0.421 |
| AlN | Wurzite -hexagonal | a=0.311, c=0.498[17] |

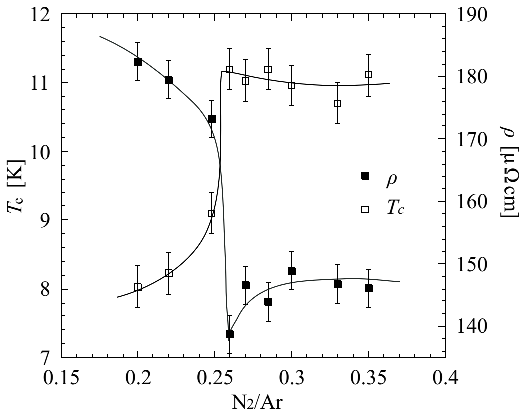


**Figure 7.** $T_c$ and $\rho$ dependence of the 8 nm NbN film on the glass wafer as a function of the $N_2$/Ar flow ratio during the deposition of the AlN buffer layer.

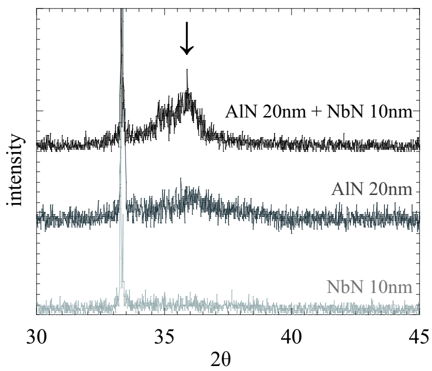


**Figure 8.** X-ray diffraction patterns from the 111 surface of NbN. Both diffractions from the 111 surface of NbN and the 002 surface of AlN appear at around $2\theta$=36.0°. The diffraction from the NbN 111 surface is not seen without the AlN buffer layer because of poor crystallinity, but it appears by introduction of the AlN buffer layer. Note that the intensity from the AlN 002 surface is much lower than that in Figure 1, because the AlN film is much thinner. The origin of the peak at 33.5° is unknown exactly, but is related to the quartz substrate.

Yusuke Sakakibara for their assistance in the experiment. This study is supported by Grant-in-Aid from the Ministry of Education, Culture, Sports, Science and Technology of Japan (15071201 and 21224002) and a collaborative research program of National Astronomical Observatory of Japan.

## References

[1] e.g. K. H. Gundlach and M. Schicke, "SIS and bolometer mixers for terahertz frequencies", *Supercond. Sci. Technol.*, **13**, R171 (2000)

[2] J. J. A. Baselmans, M. Hajenius, J. R. Gao, A. Baryshev, J. Kooi, T. M. Klapwijk, B. Voronov, P. de Korte and G. Gol'tsman, "NbN Hot Electron bolometer Mixers : Sensitivity, LO Power, Direct Detection and Stability", *IEEE Trans. Appl. Supercond.*, **15**, p.484 (2005)

[3] E. M. Gershenzon, G. N. Gol'tsman, I. G. Gogidze, Y. P. Gusev, A. I. Elantev, B. S. Karasik, and A. D. Semenov, "Millimeter and submillimeter range mixer based on electronic heating of superconductive films in the resistive state", *Sov. Phys. Supercond.*, **3**, p.1582 (1990)

[4] T. H. Courtney, J. Reintjes, and J. Wulff, "Critical Field Measurements of Superconducting Niobium Nitride", *J. Appl. Phys.*, **36**, p.660 (1965)

[5] C. M. Yen, L. E. Toth, Y. M. Shy, D. E. Anderson, and L. G. Rosner, "Superconducting $H_c$-$J_c$ and $T_c$ Measurements in the Nb-Ti-N, Nb-Hf-N, and Nb-V-N Ternary Systems", *J. Appl. Phys.*, **38**, p.2268 (1967)

[6] S. J. Lee, J. B. Ketterson, "Critical sheet resistance for the suppression of superconductivity in thin Mo-C films", *Phys. Rev. Lett.*, **64**, p.3078 (1990)

[7] S. A. Ryabchum, I. V.Tretyakov, M. I. Finkel, S. N. Maslennikov, N. S. Kaurova, V. A. Seleznev, B. M. Voronov, and G. N. Gol'tzman, "Fabrication and characterisation of NbN HEB mixers with in situ gold contacts", In Proc. 19th ISSTT, p.62 (2008)

[8] L. Jiang, S. Shiba, K. Shimbo, N. Sakai, T. Yamakura, M. Sugimura, P. G. Ananthasubramanian, H. Maezawa, Y. Irimajiri, and S. Yamamoto, "Development of THz Waveguide NbTiN HEB Mixers", *IEEE Trans. Appl. Supercond.*, **19**, p.301 (2009)

[9] Zhen Wang, Akira Kawakami, Yoshinori Uzawa, and Bokuji Komiyama, "Superconducting properties and crystal structures of single-crystal niobium nitride thin films deposited at ambient substrate temperature", *J. Appl. Phys.*, **79**, p.7837 (1996)

[10] L. Yu, R. K. Singh, Hongxue Liu, Stephen Y. Wu, Roger Hu, D. Durand, John Bulman, John M. Rowell, and Nate Newman, "Fabrication of Niobium Titanium Nitride Thin Films With High Superconducting Transition Temperatures and Short Penetration Lengths", *IEEE Trans. Appl. Supercond.*, **15**, p.44 (2005)

[11] J. R. Gao, M. Hajenius, F. D. Tichelaar, T. M. Klapwijk, B. Voronov, E. Grishin, G. Gol'tsman, C. A. Zorman, and M. Mehreegany, "Monocrystalline NbN nanofilms on a 3C-SiC/Si substrate", *APL.*, **91**, 062504 (2007)

[12] C. E. Tong, J. Stern, K. Megerian, H. LeDuc, T. K. Sridharan, H. Gibson, and R. Blundell, "A low-noise NbTiN hot electron bolometer mixer", In Proc. 12th ISSTT, p.253 (2001)

[13] D. Loudkov, C. -Y. E. Tong, R. Blundell, K. G. Megerian and J. A. Stern, "Performance of the NbTiN Hot Electron Bolometer Mixer with AlN Buffer Layer at Terahertz Frequency Range", *IEEE Trans. Appl. Supercond.*, **15**, p.476 (2005)

[14] N. N. Iosad, V. V. Roddatis, S. N. Polyakov, A. V. Varlashkin, B. D. Jackson, P. N. Dmitriev, J. R. Gao, and T. M. Klapwijk, "Superconducting transition metal nitride films for THz SIS mixers", *IEEE Trans. Appl. Supercond.*, **11**, p.3832 (2001)

[15] D. Meledin, C. -Y. E. Tong, R. Blundell, N. Kaurova, K. Smirnov, B. Voronov, and G. Gol'tsman, "Study of the IF bandwidth of NbN HEB mixers based on crystalline quartz substrate with an MgO buffer layer", *IEEE Trans. Appl. Supercond.*, **13**, p.164 (2003)

[16] T. Yamashita, K. Hamasaki, Y. Kodaira and T. Komata, "Nano-meter Bridge with Epitaxially Deposited NbN on MgO Film", *IEEE Trans. Magn.*, **MAG-21**, p.932 (1985)

[17] Hong Chen, Yongge Cao, Xianwei Xiang, "Formation of AlN nano-fibers", *J. Crystal. Growth*, **224**, p.187 (2001)